Feser, F.; Barcikowska, M.:

The influence of spectral nudging on typhoon formation in regional climate models

In: Environmental Research Letters (2012) IOP

DOI: 10.1088/1748-9326/7/1/014024

Influence of Spectral Nudging on Typhoon Formation in Regional Climate Models

Frauke Feser[1,2] and Monika Barcikowska[1,2]

[1]*Institute for Coastal Research, Helmholtz-Zentrum Geesthacht, Geesthacht, Germany*

[2]*Cluster of Excellence „Integrated Climate System Analysis and Prediction“(CliSAP) of the University of Hamburg, Germany*

Corresponding Author: Frauke.Feser@hzg.de*, Institute for Coastal Research, Helmholtz-Zentrum Geesthacht, Max-Planck-Str. 1, 21502 Geesthacht, Germany, Phone +49(0)4152 87-2816*

Short title: Spectral Nudging Impact on Typhoons in RCMs

PACS: 92.60.Qx Storms, 92.60.Aa Modeling and model calibration, 92.60.Gn Winds and their effects, 92.60.Ox Tropical meteorology, 92.70.Kb Regional climate change

Abstract

Regional climate models can successfully simulate tropical cyclones and typhoons. This has been shown and was evaluated for hindcast studies of the past decades. But often global and regional weather phenomena are not simulated at the observed location or occur too often or seldom even though the regional model is driven by global reanalysis data which constitute a near-realistic state of the global atmosphere. Therefore, several techniques were developed to make the regional model follow the global state more closely. One is spectral nudging, which is applied for horizontal wind components with increasing strength for higher model levels in this study.

The aim of this study is to show the influence this method has on the formation of tropical cyclones (TC) in regional climate models. Two ensemble simulations (each with five simulations) were computed for SE Asia and the Northwestern Pacific for the typhoon season 2004, one with spectral nudging and one without. First of all, spectral nudging reduced the overall TC number by about a factor of two. But the number of tracks which are similar to observed best track data (BTD) was highly increased. Also, spatial track density patterns were found to be more similar when using spectral nudging. The tracks merge after a short time for the spectral nudging simulations and then follow the BTD closely; for the no nudge cases the similarity is largely reduced. A comparison of seasonal precipitation, geopotential height, and temperature fields at several height levels with observations and reanalysis data showed overall a smaller ensemble spread, higher pattern correlations and reduced root mean square errors and biases for the spectral nudged simulations. Vertical

temperature profiles for selected TCs indicate that spectral nudging is not inhibiting TC development at higher levels. Both the Madden-Julian-Oscillation and monsoonal precipitation are reproduced realistically by the regional model, with results slightly closer to reanalysis data for the spectral nudged simulations. Based on this RCM hindcast study of a single typhoon season spectral nudging seems to be favorable since it has mostly positive effects on typhoon formation, location, and general circulation patterns in the generation areas of TCs.

1. Introduction

Homogeneous long-term climate data is essential for the assessment of changes in extreme events like typhoons, which are known to be associated with heavy precipitation and wind speeds. Such data is provided by global reanalyses, which often are too coarse to depict regional phenomena realistically. One way to achieve more regional detail is the dynamical regionalization using a regional climate model (RCM). Many RCM studies simulating tropical cyclones (TC) were conducted (see e.g. Cha et al., 2011, Kanamitsu et al., 2010, Feser and von Storch, 2008b, Camargo et al., 2007, Knutson et al., 2007, Walsh and Watterson, 1997), showing the ability of RCMs in reconstructing TC numbers, tracks, or intensities. Also many RCM studies exist for SE Asia (among others Zhong, 2006, Kang et al., 2005, Lee et al., 2004, Suh and Lee, 2004). But it was also shown that RCMs may deteriorate the large spatial scales when large-scale forcing is only supplied from global climate model data via the lateral boundaries (von Storch et al., 2000, Miguez-Macho et al., 2004, Waldron et al., 1996). Therefore, many RCM simulations nowadays use a spectral nudging technique which prevents the RCM to alter the global spatial scales too much in comparison to the input data (e.g. Kanamitsu et al., 2010, Knutson et al., 2007, Castro et al., 2005). Spectral nudging has also been applied successfully to RCM studies for SE Asia (Cha et al., 2011, Song et al., 2011, Yhang and Hong, 2011, Tang et al., 2010, Cha and Lee, 2009, Feser and von Storch, 2008a; 2008b).

What remains to be shown is the effect spectral nudging has on typhoon formation and associated large-scale circulation patterns. Some sensitivity experiments for a single typhoon case were shown in Feser and von Storch (2008a), but this case

study can not give answers for longer time periods. Additionally the impact of spectral nudging on meteorological fields both in the vicinity of TC generation and a larger-scale circulation is of particular interest. For this article, in addition to typhoon numbers and tracks, also large-scale circulation patterns and vertical atmospheric profiles were analysed in order to identify the effect on the middle and upper troposphere. Therefore, we simulated the typhoon season 2004 for several realizations both with and without spectral nudging and compared them to satellite data as well as to different reanalyses.

2. Model, Data, and Methods

The regional climate model used for this study is the COSMO-CLM (CCLM, www.clm-community.eu; Rockel et al., 2008; Steppeler et al., 2003). Since 2005 it is the community model of the German climate research. So far this non-hydrostatic RCM has been used for simulations on terms of up to several hundred years with spatial resolutions between 1 and 60 km. In this study, 0.5 degrees (~55 km) were selected, which corresponds to about 55 km. The model was run using the global NCEP-NCAR reanalyses I (Kalnay et al., 1996; Kistler et al, 2001, hereafter called NCEP, at a horizontal resolution of T62 (~210 km)) as boundary and initial conditions.

In CCLM, spectral nudging after von Storch et al. (2000) is implemented. Practically, the regional model solution is altered after the model computed a time step by adding an additional spectral nudging term. For this purpose, the regional model solution is transferred into spectral space via a Fourier transformation and the large spatial scales are selected by their wave numbers; the same is done for the global

reanalysis input data. Then the nudging term is determined, it depends on the difference for large spatial scales between the regional and global result. This term can be positive or negative and ‘nudges’ the regional model solution so that it becomes more similar to the large-scale input field. The nudging term is then added to the RCM result and the whole solution is transferred back to physical space. In this analysis the spectral nudging terms were added every third time step. The results are comparable to those when spectral nudging is used at every time step, but less computation time is needed. The regional spatial scales are left unchanged; the nudging is adopted only for large spatial scales and for higher model layers (above 850 hPa and with increasing strength towards higher levels as in Fig. 3 of von Storch et al., 2000) so that the regional processes close to the surface are not disturbed. In this study, the spectral nudging was applied only for the horizontal wind components. The wave numbers chosen for nudging were i=12 and j =9 which correspond to spatial scales of about 500 to 660 km; all weather phenomena larger than this were nudged. Standard parameterizations were selected and the Tiedtke convection scheme (Tiedtke, 1989) was used. The CCLM uses the SST from the NCEP reanalyses after interpolation to the high-resolution grid.

10 regional ensemble simulations were computed, 5 with (SN) and 5 without (NN) nudging. The only difference between the simulations is their starting date (consecutive days at the begin of March 2004, see Table 1). The model domain is presented in Figure 1. It was chosen to include the main typhoon generation regions in the North-Western Pacific. Therefore, TCs should mainly develop inside of the model domain and not enter the domain via its lateral boundaries. Due to the large domain, the internal model variability should be large as well (Alexandru et al., 2007).

It describes the model's ability to generate several possible atmospheric states for the same lateral boundary conditions. Spectral nudging reduces this internal model variability (Weisse and Feser, 2003) and thus leads to less differences between individual ensemble members and a smaller ensemble spread. The period analysed in this article is April-December 2004 which was quite an active typhoon season with 29 typhoons observed in the Western North Pacific.

To assess the distance between typhoons, both for simulated RCM and reference best track data (BTD) tracks, a great circle distance was computed with relaxed conditions. Both tracks had to be nearer than 500 km or less at least for 10% of the longest track's length (defined as 'overlapping'). If several CCLM tracks corresponded to the same BTD track, then only one track was counted to be overlapping. As a reference, BTD from the Japan Meteorological Agency (JMA) were used, as a former study of the authors (Barcikowska et al., 2011) proved their suitability in comparison to other BTD. For evaluation purposes observations and reanalysis data were used: TRMM satellite precipitation data (horizontal resolution 0.25˚ (~28 km)); ERA-Interim (Dee et al., 2011, horizontal resolution T255 (~80 km) and NCEP CFSR reanalysis data (Saha et al., 2010, horizontal resolution 0.5˚ (~55 km)).

A simple tracking algorithm (Feser and von Storch, 2008a) was applied to track TCs, searching for minimum sea level pressure and maximum wind speed in a distance around the track. To reduce small-scale noise and to extract weather patterns which have the size of typhoons, a digital band pass filter (Feser and von Storch, 2005) was applied to sea level pressure (SLP). The tracking criteria, which were the same for all

simulations, included that the minimum pressure had to be at least once below 995.5 hPa, and below -6.5 hPa for filtered SLP, and the maximum wind speed had to exceed 18 m/s. The tracking algorithm is calibrated to find tracks associated with typhoons, so that the result is comparable to BTD. But of course the tracking is, like other tracking algorithms, highly subjective and returns more or less track numbers dependent on how relaxed or strict the settings are chosen.

3. Results

First, the analysis will concentrate on the climatology of the simulated typhoon season. Large-scale precipitation fields, vertical temperature anomalies and the Madden-Julian oscillation (MJO) were analysed. Figure 2 shows hourly averaged summer precipitation for 2004. The CFSR analysis depicts the equatorial western Pacific monsoon and the Indian monsoon over the Bay of Bengal. The East Asia monsoon is visible for Southern China, Japan, and Korea, but slightly weaker. The RCM simulations generally show similar patterns, though the CCLM-NN ensemble mean has increased precipitation over the equatorial Pacific and at the West coast of the Philippines. This is reduced by applying spectral nudging; also the precipitation along the coast of Myanmar and over the Bay of Bengal is increased and becomes closer to the reanalysis.

The MJO is presented in Figure 3 by zonal wind speed at a height of 200 hPa for summer 2004. Shown are again the CFSR reanalyses, CCLM-NN, and CCLM-SN as ensemble mean are compared. In the beginning of July a well-defined easterly propagating disturbance of westerly winds is visible in the reanalysis. This is a phase of strong and fast propagating MJO. It is also detectable in both regional model

ensemble means. Anyhow, it is weaker for the NN case and for SN the strength is much closer to CFSR.

After the evaluation of the RCM climatology the regional simulation of typhoons is now brought into focus. The total track number and the number of tracks which match JMA best tracks for each RCM simulation is given in Table 1. Thereby it is obvious that spectral nudging leads to overall smaller track numbers, without nudging most simulations show twice as many tracks. We would like to point out that the number of tracks is a result of the tracking algorithm settings, for stricter settings track numbers found in all simulations would be reduced. Therefore, we do not draw any conclusions from the track numbers. But, even though the number of tracks found for the NN cases are quite high, they do not fulfil the great circle distance criteria compared to BTD as often as the SN simulations. In fact, for most simulations the NN ensemble shows only half or less of the overlapping tracks found for the SN ensemble.

Spatial track densities were computed and compared to the one of the JMA BTD (Table 1, last column). Pattern correlations between individual runs and BTD reveal slightly higher values (about 8%) for the spectral nudging ensemble. Figure 4 shows cumulated TC numbers for BTD and CCLM runs for each grid point, normalized by their mean spatial density fields. Overall the spatial density pattern of the SN ensemble mean is closer to BTD than the NN ensemble which shows a more outspread pattern. The individual CCLM ensemble members are shown as white contour lines for the value 3 on top of the shaded ensemble means. A higher

ensemble similarity occurs for the SN ensemble, the contour lines are close to each other. This is in contrast to the NN simulations which show a larger variability.

For typhoons found in at least 4 ensemble members for both ensembles the track patterns are presented in Figure 5. Three typhoons were found in all SN ensemble members and in 4 NN ensemble members. The SN tracks merge after a short while and then follow the observed track closely. The NN tracks do not converge and show quite differing paths which are for most cases far from the observed track. A more systematic picture for all typhoons of the 2004 typhoon season is given by Figure 6. It shows the difference (km) of simulated TC track points compared to BTD for CCLM-NN (left) and CCLM-SN (right). The size of the circles reflects the numbers of track point which were classified into distance intervals of 100 km. The colours are different for each CCLM ensemble member. Three typhoons were not tracked in any of the RCM simulations. Five typhoons were only found for SN, two only for the NN runs. The figure shows a widely spread distribution for the NN differences, extending between 0-100 and 700-800 km. For the SN runs the numbers of tracks which fit the overlapping criteria with the BTD tracks defined before are much higher (bigger circles). The track differences converge towards smaller distance intervals of 100 and 200 km and become less frequent towards larger distance intervals. This pattern suggests that the tracks shown in Figure 5 are representative for all simulated typhoons in the typhoon season 2004.

To evaluate the quality of the regional simulations seasonal atmospheric fields were compared to observational data. Before, the RCM fields were interpolated to the reference grids. Table 2 shows comparison results between ERA-Interim or TRMM

and CCLM data for summer temperature at a height of 2 meters and for seasonal (JJA) precipitation sums. For temperature, all simulated fields are very close to the reanalyses, the only difference between both ensembles is a smaller bias ensemble spread and root mean square error (rmse) ensemble spread for the SN ensemble. The precipitation fields show much larger biases and rmse, the values for SN are systematically smaller than for the NN runs, also the pattern correlations (PCs) are increased. Comparisons for temperature and geopotential height at 200 and 850 hPa between the ensemble members and CFSR reanalyses are given in Tables 3 and 4. Thereby larger similarities were found for higher atmospheric layers. Again, the SN runs show a smaller ensemble spread and higher PCs, and for most parts smaller biases and rmse. This means that if only one regional simulation is feasible, in general a SN realisation will be closer to the reference data (note that this is the high-resolution NCEP CFSR, not the coarse NCEP I which was used as input for the RCM simulations) than a NN simulation.

To understand the effect spectral nudging has both on surface and higher atmospheric layers vertical temperature anomalies profiles for the most intense phase of typhoon Tingting are presented in Figure 7. The plots show vertical temperature anomalies averaged over the radial distance from the TC centre. Thereby the most intense phase was chosen as the phase with maximum TC wind speed (plus and minus one day) along Tingting's track for each simulation, this means that often different dates were taken. This was done in order to extract the most intense typhoon period, not accounting for a possible faster or slower typhoon development or a small displacement in the individual realizations. The CFSR reanalysis shows the warm core and relatively colder adjacent areas around it. For

the regional simulations the ensemble mean was plotted as shaded colours with isolines for each ensemble member on top of it. The typhoon was found in 4 ensemble members of CCLM-SN, but in only 2 members of CCLM-NN. Even for these two members larger differences are visible, but the ensemble mean is still quite similar to CFSR. As can be seen, spectral nudging decreases the ensemble spread also in this case, the isolines of the 4 ensemble members are very close to each other. The RCM simulations show temperature anomalies that extend down to the surface in contrast to the CFSR reanalysis. This is even more obvious for the SN cases. The temperature anomalies are even a little more extreme for SN than for NN. This indicates that SN does not inhibit typhoon development in this case study. A comparable result was found for typhoons Songda and Megi, while for Namtheun the NN members showed slightly stronger anomalies (also stronger than CFSR, not shown).

Horizontal wind fields for typhoon Songda are presented in Figure 8. The left panel shows the CFSR reanalysis with a well-developed typhoon including an eye and the eye wall. The middle and right part of the figure depict the RCM results for the NN and SN ensemble, respectively. The underlying shaded pattern is the first ensemble member, while the other members are given as contour lines of 10 (solid lines) and 18 m/s (dotted lines). The intention to choose the first ensemble members nos. 10 and 20 as shaded patterns, no matter which quality they would have, was that normally when running an RCM simulation there would be no ensemble, but only a single run. Therefore there would not be a chance to choose e.g. the best-fitting simulation. For the SN cases, the contour lines are close to each other and resemble the underlying pattern which reflects the large similarity between all SN simulations.

In comparison to the reanalysis the typhoon location is quite similar, wind speed is weaker, but an eye and eye wall evolve. Cha et al. (2011) recently showed that spectral nudging can reduce typhoon intensities due to disturbing the TC development process especially at higher model levels, since spectral nudging is normally applied here with more strength than for lower levels. This effect may also take place here, leading to reduced typhoon near-surface wind speeds for the typhoon intensification phase. For the peak phase SN shows higher wind speeds than the NN simulations (not shown).

The NN runs show very differing patterns. Even though some intense typhoons were simulated they are all located at different places and none of them resembles the reanalysis. This is also shown by the contour lines which are distributed over the whole area. The same can be seen for precipitation fields of typhoon Ma-on, given in Figure 9. While the SN ensemble shows again a small ensemble spread and large similarity to the reanalysis (though shifted slightly to the South), the NN runs are very different and most of them are not close to the CFSR reanalysis. There is one simulation (shown as contour lines) which shows high precipitation values comparable to CFSR, shifted to the southwest, but the other ones do not show any high precipitation. When running a long simulation without nudging the chance would be small to pick the simulation which would be nearest to observations. This is in accordance with earlier results of Weisse and Feser (2003) and Alexandru et al. (2009) which showed that the internal RCM variability is reduced by applying spectral nudging.

4. Summary and Conclusions

This article examined the effect of spectral nudging on TC development in RCMs. Ensemble studies were computed using either spectral nudging or a standard forcing via the lateral RCM boundaries. The greatest impact was found for the number, location and path of TCs. Spectral nudging decreases the total TC number, but in contrast the similarity of the remaining TC tracks with BTD is enhanced. This also leads to larger pattern correlations with BTD for TC spatial densities and associated atmospheric patterns. The tracks of the spectral nudged simulations converge shortly after their appearance and then stay close to the BTD paths, this is in contrast to the non-nudged simulations which show large deviations. For most SN ensemble members a higher pattern correlation and a reduced bias and root-mean-square error was found for precipitation, near-surface temperature, and for both temperature and geopotential height at higher levels. The ensemble spread is reduced for the spectral nudging cases. A comparison of vertical temperature profiles for several typhoons did not show large differences between the two ensembles, indicating that SN did not inhibit the vertical TC development for these cases. But these were only selected case studies and this should be studied in more detail since Cha et al. (2011) reported reduced TC intensities and disturbed TC intensification processes caused by SN. Large-scale circulation patterns like monsoonal precipitation or the Madden-Julian oscillation were not disturbed, but became slightly closer to high-resolution reanalysis data for the SN runs.

The added value of regional climate modelling and the use of spectral nudging depend strongly on the type of application (Feser et al., 2011). For hindcasts that aim at a description of the past atmospheric state it is desirable to reconstruct TCs and

the according circulation patterns as realistic as possible. Simulated TCs will on average be closer to observations or high-resolution reanalysis data when using spectral nudging. Since spectral nudging mainly improves the location of TCs this leads to larger similarities for typhoon tracks and related atmospheric patterns in comparison to observations. Also general circulation patterns become closer to observations or to high-resolution reanalyses, not just for higher model levels but in addition close to the surface. For TC sensitivity studies that deal with analysing TC intensification processes spectral nudging may not be suitable. Thus, we recommend the application of spectral nudging for hindcast studies that should stay close to observed values, like e.g. the generation of multi-decadal, regional, and homogeneous data sets that may be used for statistical analysis of changes in storm climate.

Acknowledgments

The authors thank B. Gardeike for her help with the preparation of the figures for this paper. The COSMO-CLM is the community model of the German climate research (www.clm-community.eu). The German Climate Computing Center (DKRZ) provided the computer hardware for the LAM simulations in the project 'Regional Atmospheric Modelling'. The NCEP/NCAR reanalysis data was provided by the National Center for Atmospheric Research (NCAR). The CFSR data was developed by NOAA's National Centers for Environmental Prediction (NCEP). The ERA-Interim data are from NOAA's National Operational Model Archive and Distribution System (NOMADS) which is maintained at NOAA's National Climatic Data Center (NCDC). The 'best track data' were made available by the Japan Meteorological Agency (JMA). The TRMM data used in this study were acquired as part of the activities of

NASA's Science Mission Directorate, and are archived and distributed by the Goddard Earth Sciences (GES) Data and Information Services Center (DISC). The work was supported (in parts) through the Cluster of Excellence 'CliSAP', University of Hamburg, funded through the German Science Foundation (DFG-EXC177). This work is a contribution to the Helmholtz Climate Initiative REKLIM (Regional Climate Change), a joint research project of the Helmholtz Association of German research centres (HGF). We thank the two anonymous reviewers for their constructive comments.

References

Alexandru, A., R. de Elia, R. Laprise, L. Separovic, and S. Biner: 2009: Sensitivity Study of Regional Climate Model Simulations to Large-Scale Nudging Parameters. *Mon. Wea. Rev.*, **137**, 1666-1686, DOI: 10.1175/2008MWR2620.1.

Alexandru, A., R. de Elia, and R. Laprise, 2007: Internal Variability in Regional Climate Downscaling at the Seasonal Scale. *Mon. Wea. Rev.*, **135**, 3221-3238, DOI: 10.1175/MWR3456.1.

Barcikowska, M., F. Feser and H. von Storch, 2011: Usability of best track data in climate statistics in the western North Pacific. Submitted to *Mon. Wea. Rev.*

Camargo, S. J., H. L. Li, and L. Q. Sun, 2007: Feasibility study for downscaling seasonal tropical cyclone activity using the NCEP regional spectral model. *Int. J. Climatol.*, **27**(3), 311–325, doi:10.1002/joc.1400.

Castro, C. L., R. A. Pielke Sr., and G. Leoncini, 2005: Dynamical downscaling: Assessment of value retained and added using the Regional Atmospheric Modeling System (RAMS). *J. Geophys. Res*., **110**, D05108, doi:10.1029/2004JD004721.

Cha, D. H., C. S.Jin, D. K. Lee, and Y. H. Kuo, 2011: Impact of intermittent spectral nudging on regional climate simulation using Weather Research and Forecasting model. *J. Geophys. Res*., **116**, DOI: 10.1029/2010JD01506.

Cha, D. H., D. K. Lee, 2009: Reduction of systematic errors in regional climate simulations of the summer monsoon over East Asia and the western North Pacific by applying the spectral nudging technique. *J. Geophys. Res*., **114**, DOI: 10.1029/2008JD011176

Dee, D. P., and Coauthors, 2011: The ERA-Interim reanalysis: Configuration and performance of the data assimilation system. *Quart. J. R. Meteorol. Soc.*, **137**, 553-597. DOI:10.1002/qj.828.

Feser, F., B. Rockel, H. von Storch, J. Winterfeldt, and M. Zahn, 2011: Regional Climate Models add Value to Global Model Data: A Review and selected Examples. *Bull. Amer. Meteor. Soc.*, doi: 10.1175/2011BAMS3061.1., 92 (9), pp. 1181-1192.

Feser, F., and H. von Storch, 2008a: A dynamical downscaling case study for typhoons in SE Asia using a regional climate model. *Mon. Wea. Rev.*, 136 (5), 1806-1815.

Feser, F., and H. von Storch, 2008b: Regional modelling of the western Pacific typhoon season 2004. *Meteor. Z.*, **17**, 4, 519-528.

Feser, F., and H. von Storch, 2005: A spatial two-dimensional discrete filter for limited area model evaluation purposes. *Mon. Wea. Rev.*, **133**(6), 1774-1786.

Kalnay, E., and Coauthors, 1996: The NCEP/NCAR reanalysis project. *Bull. Amer. Meteor. Soc.* **77**, 437–471.

Kanamitsu, M., K. Yoshimura, Y.-B. Yhang, and S.-Y. Hong, 2010: Errors of Interannual Variability and Trend in Dynamical Downscaling of Reanalysis, *J. Geophys. Res., 115,* D17115, doi:10.1029/2009JD013511.

Kang, H. S., D. H. Cha, and D. K. Lee, 2005: Evaluation of the mesoscale model/land surface model (MM5/LSM) coupled model for East Asian summer monsoon simulations. *J. Geophys. Res.*, **110**, D10105, doi:10.1029/2004JD005266.

Kistler, R., E. Kalnay, W. Collins, S. Saha, G. White, J. Woollen, M. Chelliah, W. Ebisuzaki, M. Kanamitsu, V. Kousky, H. van den Dool, R. Jenne, and M. Fiorino, 2001: The NCEP–NCAR 50-Year Reanalysis: Monthly Means CD-ROM and Documentation. *Bull. Amer. Meteor. Soc.*, **82**, 247-267.

Knutson, T., J. Sirutis, S. Garner, I. Held, R. Tuleya, 2007: Simulation of the Recent Multidecadal Increase of Atlantic Hurricane Activity Using an 18-km-Grid Regional Model, *Bull. Amer. Meteor. Soc.*, **88**, 1549–1565.

Lee, D. K., D. H. Cha, and H. S. Kang, 2004: Regional climate simulation of the 1998 summer flood over East Asia. *J. Meteorol. Soc. Jpn.*, **82**(6), 1735–1753, doi:10.2151/jmsj.82.1735.

Miguez-Macho, G., G. L. Stenchikov, and A. Robock, 2004: Spectral nudging to eliminate the effects of domain position and geometry in regional climate model simulations. *J. Geophys. Res.*, **109**, D13104, 10.1029/2003JD004495.

Rockel, B, A. Will, and A. Hense, 2008: The Regional Climate Model COSMO-CLM (CCLM). Editorial, *Meteor. Z*., **12**, 4, 347-348.

Saha, S., and Coauthors, 2010: The NCEP Climate Forecast System Reanalysis. *Bull. Amer. Meteor. Soc.*, **91**, 1015–1057. doi: 10.1175/2010BAMS3001.1

Song, S., J. P. Tang, X. Chen, 2011: Impacts of Spectral Nudging on the Sensitivity of a Regional Climate Model to Convective Parameterizations in East Asia. *Acta Meteorologica Sinica*, **25**, 63-77, DOI: 10.1007/s13351-011-0005-z.

Steppeler, J., G. Doms, U. Schättler, H. W. Bitzer, A. Gassmann, U. Damrath, and G. Gregoric, 2003: Meso-gamma scale forecasts using the nonhydrostatic model LM. *Meteor. Atm. Phys.*, **82**, 75-96.

Suh, M. S., and D. K. Lee, 2004: Impacts of land use/cover changes on surface climate over east Asia for extreme climate cases using RegCM2. *J. Geophys. Res.*, **109**, D02108, doi:10.1029/2003JD003681.

Tang, J. P., S. Song, J. A. Wu, 2010: Impacts of the spectral nudging technique on simulation of the East Asian summer monsoon. *Theoretical and Applied Climatology*, **101**, 41-51, DOI: 10.1007/s00704-009-0202-1.

Tiedtke, M., 1989: A Comprehensive Mass Flux Scheme for Cumulus Parameterization in Large-Scale Models. *Mon. Wea. Rev.* **117**, 1779–1800.

von Storch, H., H. Langenberg, and F. Feser, 2000: A Spectral Nudging Technique for Dynamical Downscaling Purposes, *Mon. Wea. Rev.*, **128**, 10, 3664-3673.

Waldron, K. M., J. Paegle, and J. D. Horel, 1996: Sensitivity of a spectrally filtered and nudged limited-area model to outer model options. *Mon. Wea. Rev.,* **124,** 529–547.

Walsh K. J., I. G. Watterson, 1997: Tropical cyclone-like vortices in a limited area model: comparison with observed climatology. *J. Clim*. **10**, 2240–2259.

Weisse, R. and F. Feser, 2003: Evaluation of a method to reduce uncertainty in wind hindcasts performed with regional atmosphere models. *Coastal Engineering*, **48**, 211-225.

Yhang, Y. B., and S. Y. Hong, 2011: A study on large-scale nudging effects in regional climate model simulation. *APJAS*, **47**, 235-243, DOI: 10.1007/s13143-011-0012-0.

Zhong, Z., 2006: A possible cause of a regional climate model's failure in simulating the east Asian summer monsoon. *Geophys. Res. Lett.*, **33**, L24707, doi:10.1029/2006GL027654.

Figure Captions List

Figure 1 Model domain and surface elevation (m) of the RCM ensemble simulations for Southeast Asia and the Northwestern Pacific. The grid distance is 0.5 x 0.5 degrees which corresponds to about 55 x 55 km.

Figure 2 Total hourly averaged precipitation [mm] for JJA 2004 for NCEP CFSR (left), CCLM-NN ensemble mean (middle) and CCLM-SN ensemble mean (right).

Figure 3 Hovmöller diagram of the Madden-Julian oscillation represented by zonal wind speed [m/s] at a height of 200hPa for JJA 2004, averaged from 5ºS to the equator. Shown are NCEP CFSR (left) as well as CCLM-NN (middle) and CCLM-SN (right) ensemble means.

Figure 4 TC spatial densities (TC occurrence per year and grid point; normalized by the mean spatial density fields) for BTD, CCLM-NN, and CCLM-SN. For CCLM the ensemble mean is shown is shaded, the individual simulations are shown as white contour lines for the value 3.

Figure 5 Tracks of Typhoon Namtheun 200410 (left), Songda, 200418 (middle), and Ma-on 200422 (right), as given by best track data of JMA (black), RCM simulations with (red) and without (blue) spectral nudging.

Figure 6 Difference of simulated TCs compared to BTD for the year 2004 for CCLM-NN (left) and CCLM-SN (right). The y-axis shows the individual TC IDs, those TCs

which were not tracked in either NN or SN simulations were omitted (3, 11, 26). The size of the circles on the x-axis gives the number of track points classified into distance intervals of 100 km. The different colours depict the individual CCLM ensemble members.

Figure 7 Vertical temperature anomalies [K] averaged over the radial distance [km] from the TC center for typhoon Tingting at its stage with maximum near-surface wind speed plus and minus one day for NCEP CFSR (left), and each of the CCLM-NN (middle) and CCLM-SN (right) simulations. Shown are isolines for plus and minus 1 K. For CCLM the shaded areas show the ensemble mean and isolines are depicted for all ensemble members which included the typhoon at that time in a circular distance to JMA BTD of no more than 550 km (2 members for CCLM-NN and 4 for CCLM-SN).

Figure 8 Horizontal 10m wind speed fields (m/s) for typhoon Songda (200418), on September 1st 2004, 0:00. From left: CFSR reanalysis, CCLM-NN, CCLM-SN. For CCLM the first simulation (simulation nos. 10 and 20) of each ensemble is shaded, the other simulations are shown as contour lines: 10 m/s as solid lines, 18 m/s as dotted lines.

Figure 9 Precipitation (daily sum, mm) for typhoon Ma-on (200422) on October 8, 2004, close to Japan. From left: CFSR reanalysis, CCLM-NN, CCLM-SN. For CCLM the first simulation (simulation nos. 10 and 20) of each ensemble is shaded, the other simulations are shown as contour lines: 40 mm as solid lines, 120 mm as dotted lines.

Tables

Table 1

The table shows the regional climate simulation ID, if spectral nudging was used, the simulation start date, the total track number and the number of tracks which match JMA best tracks. The last column shows the spatial pattern correlation between spatial track densities of the individual CCLM simulations and the JMA BTD. The simulations were all started at 12:00 a.m., the only difference between simulations 10-14 (without spectral nudging) and between runs 20-24 (with spectral nudging) is the starting date.

Simulation ID	Spectral Nudging	Start Date	Total Track Number	Overlapping Tracks	PC SPD
10	No	03/01/2004	66	12	0.50
11	No	03/02/2004	65	10	0.59
12	No	03/03/2004	65	9	0.61
13	No	03/04/2004	64	7	0.55
14	No	03/05/2004	62	10	0.57
20	Yes	03/01/2004	40	21	0.67
21	Yes	03/02/2004	31	20	0.61
22	Yes	03/03/2004	31	22	0.64
23	Yes	03/04/2004	29	19	0.66
24	Yes	03/05/2004	28	20	0.64

Table 2

Comparison to observation data: Seasonal (JJA) summed precipitation of RCM compared to TRMM data and seasonal (JJA) averaged near-surface temperature compared to ERA-Interim reanalysis. Shown are pattern correlations (PC), bias and root-mean square errors (RMSE).

Simulation ID	PC TOT_PREC	BIAS Precip	RMSE Precip	PC T_2M	BIAS T_2M	RMSE T_2M
10	0.58	94.16	434.50	0.99	-0.29	1.22
11	0.58	88.51	422.53	0.99	-0.28	1.24
12	0.58	86.58	437.33	0.99	-0.16	1.05
13	0.60	89.94	437.07	0.99	-0.15	1.07
14	0.57	90.13	437.95	0.99	-0.09	1.01
20	0.67	49.34	316.23	0.99	-0.24	1.03
21	0.66	49.07	320.40	0.99	-0.25	1.04
22	0.68	48.80	311.53	0.99	-0.25	1.04
23	0.67	48.76	316.58	0.99	-0.25	1.05
24	0.68	48.57	315.10	0.99	-0.24	1.05

Table 3

Comparison to high-resolution reanalysis data: Seasonal (JJA) mean RCM temperature at 200 and 850 hPa compared to NCEP CFSR reanalysis. Shown are pattern correlations (PC), bias and root-mean square errors (RMSE).

Simulation ID	PC T 200hPa	BIAS T200	RMSE T200	PC T850	BIAS T850	RMSE T850
10	0.89	0.64	1.14	0.90	-0.65	2.00
11	0.89	0.73	1.22	0.89	-0.59	2.01
12	0.92	0.50	0.97	0.91	-0.49	1.82
13	0.92	0.45	0.95	0.90	-0.42	1.80
14	0.91	0.53	1.02	0.90	-0.36	1.81
20	0.94	0.16	0.71	0.91	-0.54	1.75
21	0.94	0.16	0.70	0.91	-0.55	1.75
22	0.94	0.15	0.71	0.91	-0.54	1.75
23	0.94	0.15	0.70	0.91	-0.54	1.75
24	0.93	0.15	0.71	0.91	-0.55	1.75

Table 4

Comparison to high-resolution reanalysis data: Seasonal (JJA) mean RCM geopotential height at 200 and 850 hPa compared to NCEP CFSR reanalysis. Shown are pattern correlations (PC), bias and root-mean square errors (RMSE).

Simulation ID	PC FI200hPa	BIAS FI200	RMSE FI200	PC FI850	BIAS FI850	RMSE FI850
10	0.99	-8.06	23.68	0.88	-13.06	21.42
11	0.99	-13.06	28.76	0.88	-17.78	24.48
12	0.99	-0.64	18.52	0.88	-8.62	19.90
13	0.99	-1.39	18.26	0.88	-10.37	19.76
14	0.99	1.70	23.95	0.84	-8.87	22.58
20	1.00	1.15	15.64	0.97	-3.18	9.85
21	1.00	1.03	15.51	0.97	-3.18	9.81
22	1.00	0.87	15.59	0.97	-3.04	9.86
23	1.00	0.94	15.55	0.97	-3.10	9.85
24	1.00	0.99	15.63	0.97	-3.14	9.82

Figures

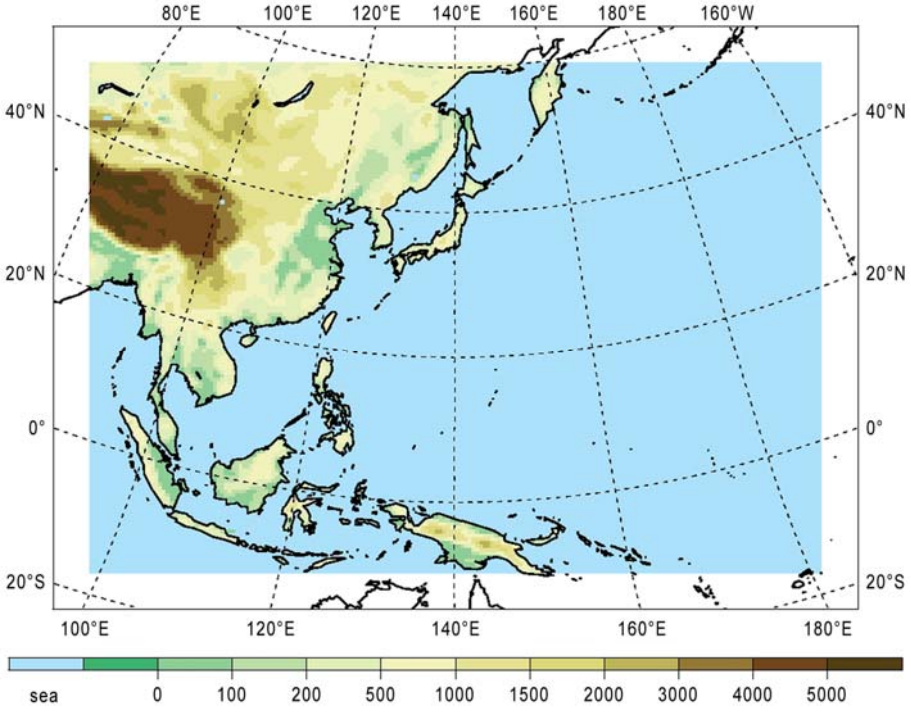

Figure 1 Model domain and surface elevation (m) of the RCM ensemble simulations for Southeast Asia and the Northwestern Pacific. The grid distance is 0.5 x 0.5 degrees which corresponds to about 55 x 55 km.

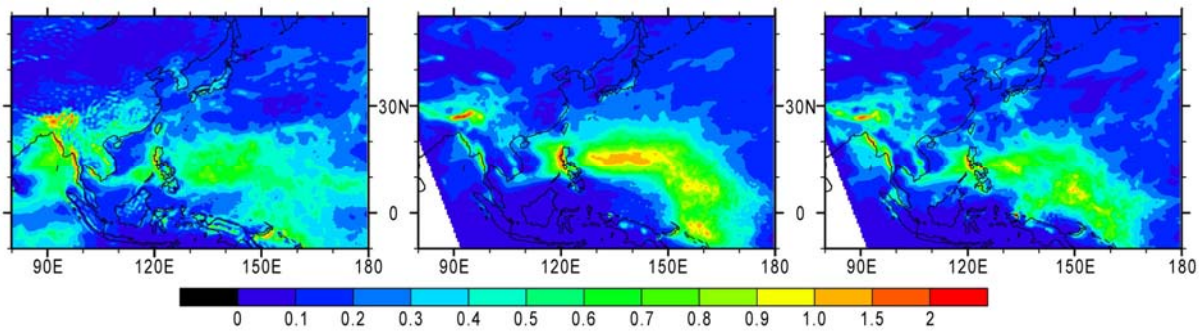

Figure 2 Total hourly averaged precipitation [mm] for JJA 2004 for NCEP CFSR (left), CCLM-NN ensemble mean (middle) and CCLM-SN ensemble mean (right).

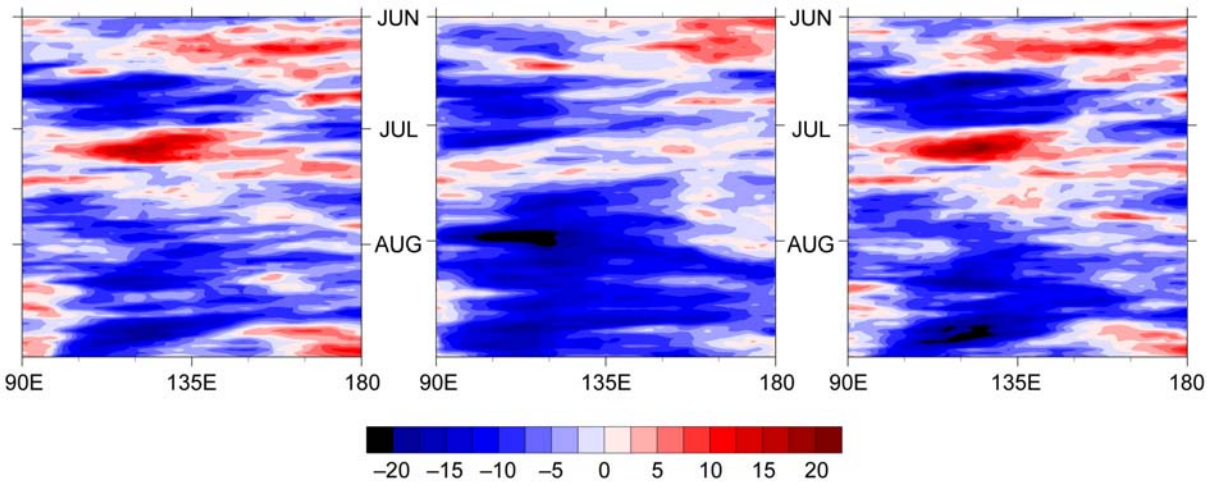

Figure 3 Hovmöller diagram of the Madden-Julian oscillation represented by zonal wind speed [m/s] at a height of 200hPa for JJA 2004, averaged from 5ºS to the equator. Shown are NCEP CFSR (left) as well as CCLM-NN (middle) and CCLM-SN (right) ensemble means.

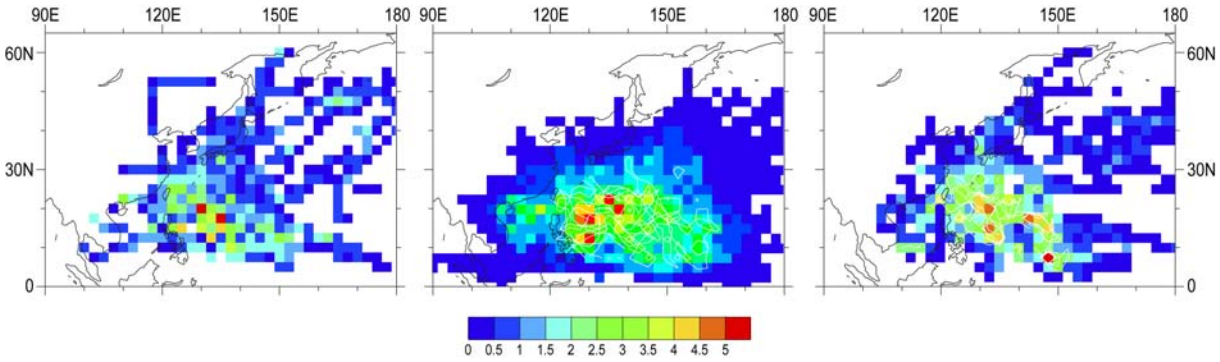

Figure 4 TC spatial densities (TC occurrence per year and grid point; normalized by the mean spatial density fields) for BTD, CCLM-NN, and CCLM-SN. For CCLM the ensemble mean is shaded, the individual simulations are shown as white contour lines for the value 3.

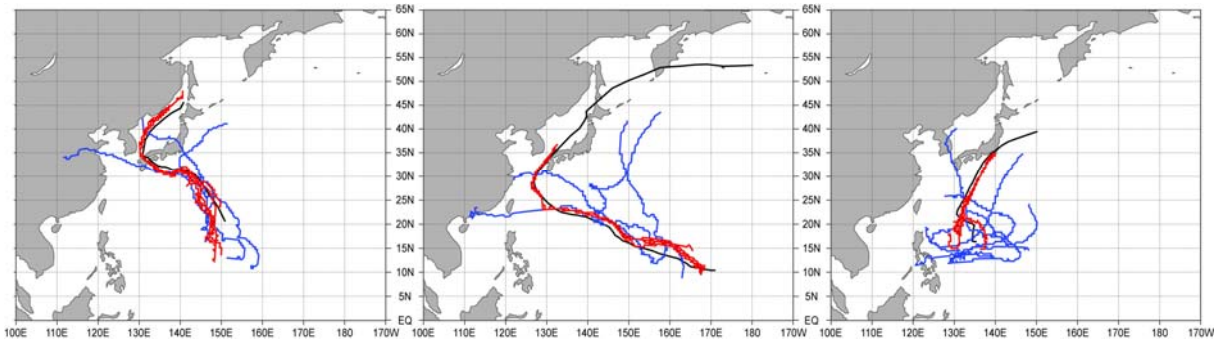

Figure 5 Tracks of Typhoon Namtheun 200410 (left), Songda, 200418 (middle), and Ma-on 200422 (right), as given by best track data of JMA (black), RCM simulations with (red) and without (blue) spectral nudging.

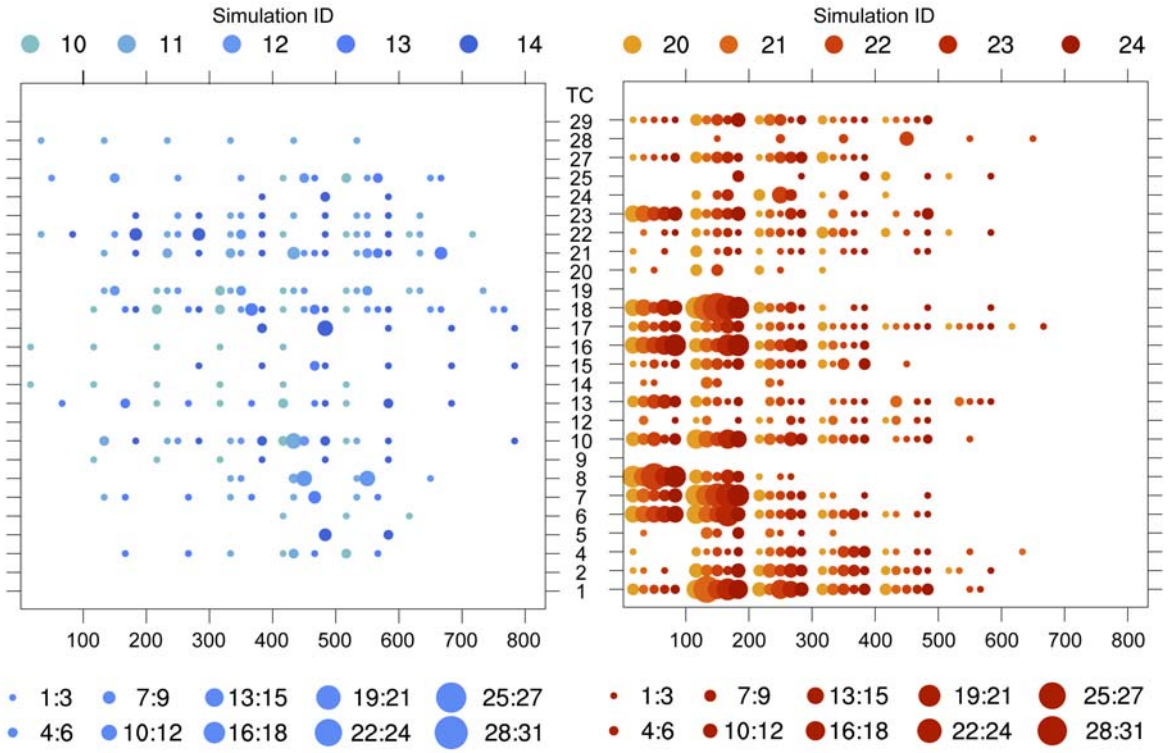

Figure 6 Difference of simulated TCs compared to BTD for the year 2004 for CCLM-NN (left) and CCLM-SN (right). The y-axis shows the individual TC IDs, those TCs which were not tracked in either NN or SN simulations were omitted (3, 11, 26). The size of the circles on the x-axis gives the number of track points classified into distance intervals of 100 km. The different colours depict the individual CCLM ensemble members.

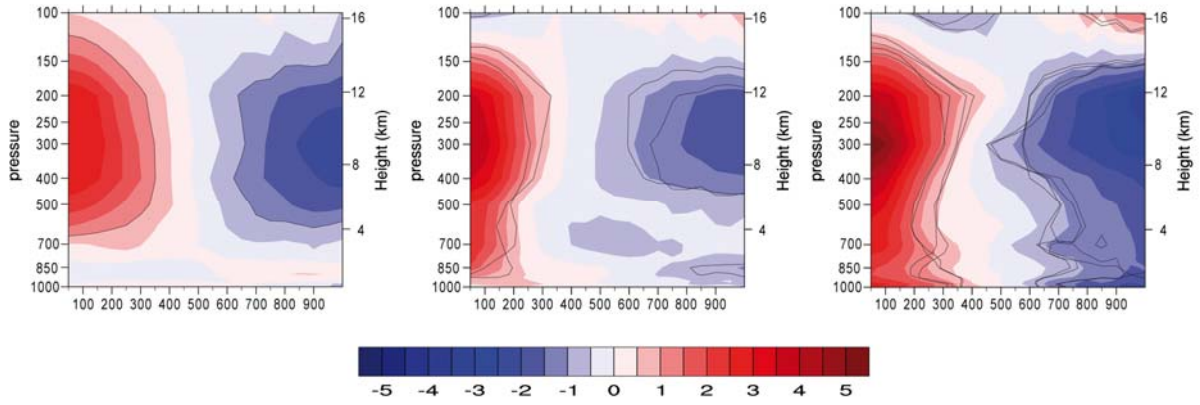

Figure 7 Vertical temperature anomalies [K] averaged over the radial distance [km] from the TC center for typhoon Tingting at its stage with maximum near-surface wind speed plus and minus one day for NCEP CFSR (left), and each of the CCLM-NN (middle) and CCLM-SN (right) simulations. Shown are isolines for plus and minus 1 K. For CCLM the shaded areas show the ensemble mean and isolines are depicted for all ensemble members which included the typhoon at that time in a circular distance to JMA BTD of no more than 550 km (2 members for CCLM-NN and 4 for CCLM-SN).

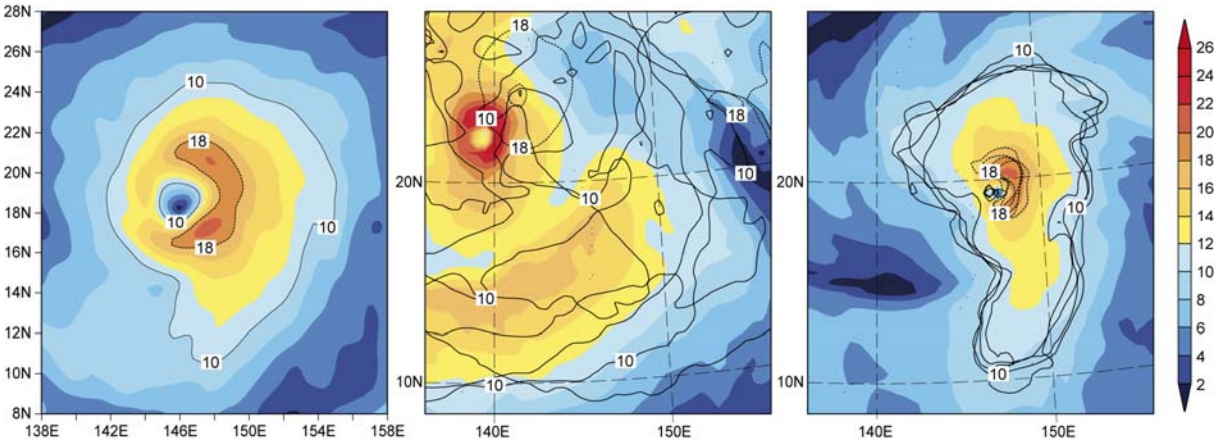

Figure 8 Horizontal 10m wind speed fields (m/s) for typhoon Songda (200418), on September 1st 2004, 0:00. From left: CFSR reanalysis, CCLM-NN, CCLM-SN. For CCLM the first simulation (simulation nos. 10 and 20) of each ensemble is shaded, the other simulations are shown as contour lines: 10 m/s as solid lines, 18 m/s as dotted lines.

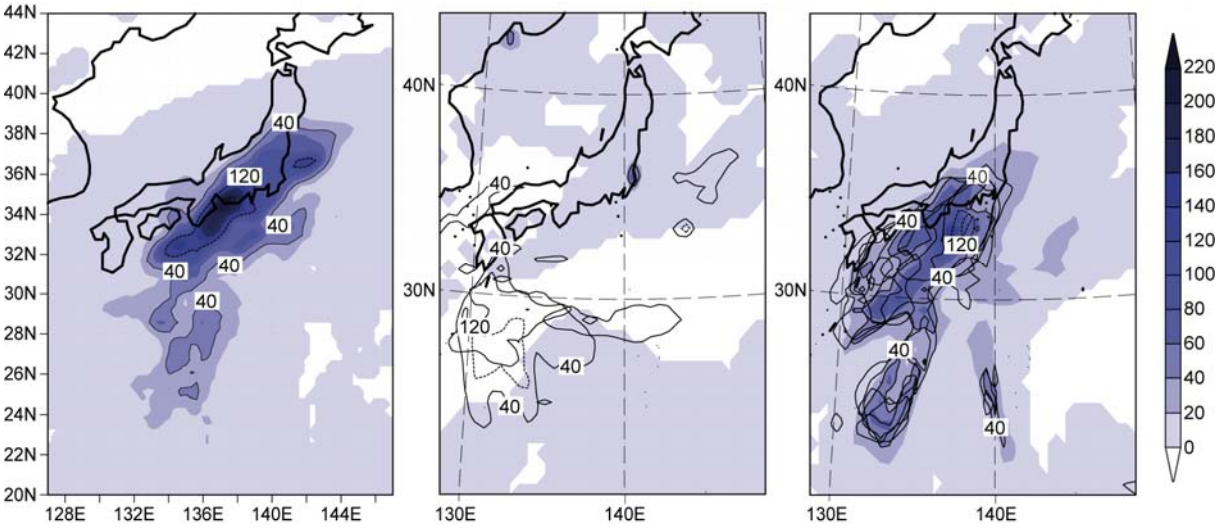

Figure 9 Precipitation (daily sum, mm) for typhoon Ma-on (200422) on October 8, 2004, close to Japan. From left: CFSR reanalysis, CCLM-NN, CCLM-SN. For CCLM the first simulation (simulation nos. 10 and 20) of each ensemble is shaded, the other simulations are shown as contour lines: 40 mm as solid lines, 120 mm as dotted lines.